Verlag Ferdinand Berger & Söhne Ges.m.b.H., Horn, Austria, download unter www.biologiezentrum.

Image processing in taxonomy*

G. Newton & B. Kendrick

Department of Biology, University of Waterloo, Waterloo, Ontario, Canada N2L 3G1

Newton, G. & B. Kendrick (1990). Image processing in taxonomy. – Sydowia 42: 246–272.

Image processing techniques and computers have advanced to a level where their use in taxonomy is feasible both technically and economically. Automated measurement of traditional features, as well as the possibility of new features only extractable by computer, make this a dynamic area of research. In this paper, fungal spores, diagnostic structures in fungal taxonomy, are the subject of general image processing algorithms, as well as a specific algorithm for the extraction of spore shape.

In the identification and classification of fungi (and other organisms), taxonomists have traditionally manually extracted simple quantitative measures (length, width, etc.) of structures such as conidia, as well as categorizing them visually by their shape (i.e. ellipsoidal). These two methods of extracting features are at opposite ends of the spectrum, both in the information they provide and in the way they are measured: quantitative measures such as length and width are conceptually simple and objective (though observer error varies greatly), but do not convey very much information about the subject; in contrast, shape is a complex, information-dense, sometimes subjective measure conveying a more complete idea of the subject. This dichotomy of measures, characterized by the inadequacy of the quantitative and the complexity of the qualitative, has resulted from the difficulties involved with the measurement of features pertaining to shape. Such measures exist, but tend to use more information than could realistically be manually extracted, such as the position of every point of the outline of the subject, or all the points contained by the outline. Measures which do compress large amounts of information about shapes have been developed in the area of **Image Processing**, where they have already been used in the identification of man-made objects, such as machine parts. These measures **or shape descriptors** range from simple perimeter-to-surface relationships, shape eccentricity and compactness, to various

* Paper based on a talk given at the Fourth International Mycological Congress, Symposium G-6, Techniques and Instrumentation in Mycology, held in Regensburg, FRG, 28th August – 3rd September 1990.

Verlag Ferdinand Berger & Söhne Ges.m.b.H., Horn, Austria, download unter www.biologiezentrum.

complex shape descriptors involving central moments and Fourier analysis (PERSOON & FU, 1977; PAVLIDIS, 1978; BALLARD & BROWN, 1982; GONZALEZ & WINTZ, 1987). As well as allowing for the extraction of more complex shape descriptors, Image Analysis may also automate the extraction of the traditional measures (length, width) allowing more samples to be measured and a more statistical representation of these measures to be made (i.e. as opposed to measuring 20 lengths and widths manually, an automated system may measure

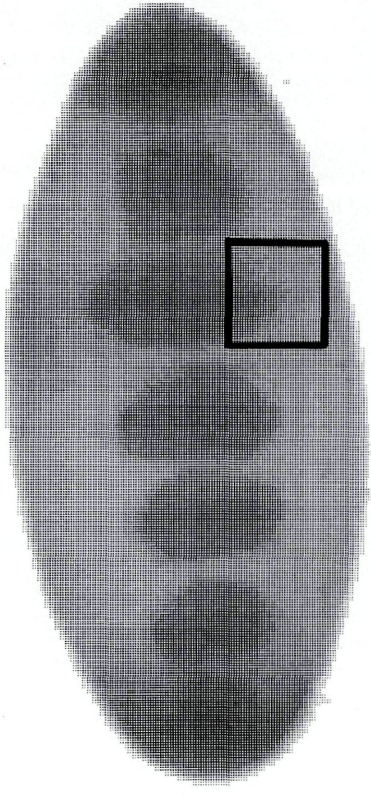

Fig. 1A – Digitized *Bipolaris conidium* (400X, 224x200 pixels). Details of block shown in Fig.1B.

Verlag Ferdinand Berger & Söhne Ges.m.b.H., Horn, Austria, download unter www.biologiezentrum.

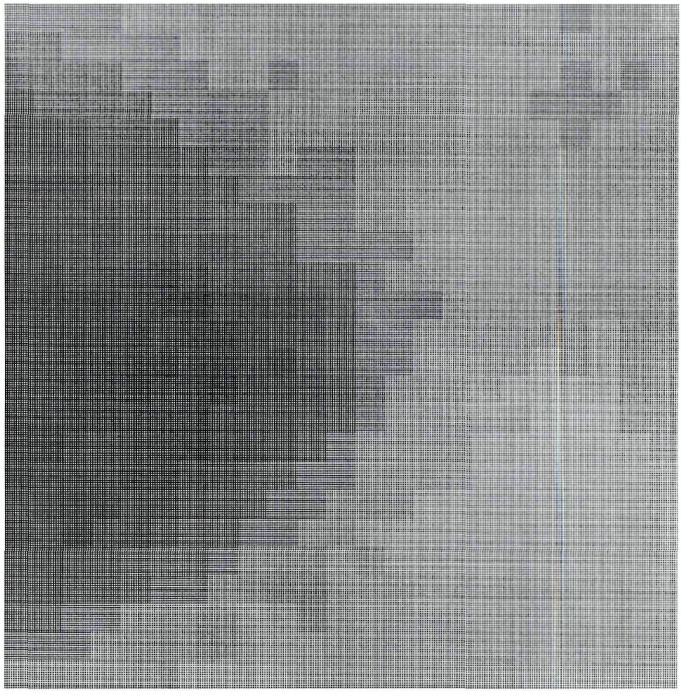

Fig. 1B – Close-up of Fig.1A, showing digital nature of the image. (24x23 pixels).

500 lengths and widths, allowing a statistically useful mean and standard deviation to be calculated).

The first stage in Image Processing is the transformation of the continuous analog image produced by a television camera into a digital form usable by the computer. The digitization process overlays a square or rectangular grid onto the image, takes the average image brightness inside each grid cell (or pixel) and assigns this brightness level to the cell (Fig. 1). For gray-scale image processing, which is the dominant form of image processing, the image sensor (i.e. black and white camera) samples across the visible light frequencies to obtain the brightness level. (In colour image processing, three separate areas of the visible spectrum [red, green, blue] are sampled and three respective brightnesses are recorded for each

Verlag Ferdinand Berger & Söhne Ges.m.b.H., Horn, Austria, download unter www.biologiezentrum.

pixel). Brightness is recorded as an integer ranging from 0, black, to 255 (or some power of 2, such as 16, 32, 64), which is completely saturated with the frequency that is being measured. The imposition of a discrete grid onto the continuous image introduces what is known as digitization error. Digitization error is dependent on the size of the grid and the orientation and nature of the subject, and introduces a certain amount of distortion into the digital version of the image. Electronic noise, akin to that found corrupting transmitted television images, is also introduced by each electrical component of the system, and even the level of insulation on the cabling connecting the camera to the digitizer affects the image quality.

Because a certain amount of unwanted noise and distortion may exist in the digitized image, preprocessing of the image may be necessary before any feature extraction takes place. Preprocessing methods often involve image enhancement and image restoration, which attempt to suppress noise and improve image quality, often with some specific feature in mind. Fig. 2 shows two simple preprocessing techniques: image smoothing, used to reduce noise; and image sharpening, which uses a Laplacian-based filter. Unfortunately, these two techniques tend to have complementary undesirable side effects: image smoothing blurs edges (Fig. 2B) and sharpening accentuates noise (Fig. 2C).

Once the digital image is produced, the development of an image analysis system for the identification of any structure must begin with the segmentation of the image in order to extract features from the subject. Segmentation is the separation of the subject(s) from the background to permit subsequent analysis on the subject (Fu & Mui, 1981; Haralick & Shapiro, 1985). One common method is called **thresholding** (Sahoo & al. 1985). This is a global technique which examines the distribution of the gray levels and tries to choose a brightness level which divides the foreground subject from the background. This requires that there be a certain amount of contrast between the subject and the background. This method is effective if the structures or organisms are consistently pigmented and substantially darker or lighter than the background but much less effective in fungi which are often colourless or variably pigmented and septate.

Another segmentation technique is **edge detection** which, unlike thresholding, has some basis in mammalian vision systems (Marr & Hildreth, 1980; Granrath, 1981; Hildreth, 1983; Watt, 1987). Edge detection is sensitive to relative changes at a local level, usually associated with the boundaries of shapes and regions. When moving from the subject to the background, a shift in the gray levels can be detected, and this is associated with the subject's outline. As it is a local method, edge detection tends to retain more detail – and noise –

Verlag Ferdinand Berger & Söhne Ges.m.b.H., Horn, Austria, download unter www.biologiezentrum.

Fig. 2A – Digitized *Podospora* ascospore (1000x, 200x160 pixels).

than thresholding. A plethora of different edge detectors have been developed (BALLARD & BROWN, 1982; HARALICK, 1984) with different mathematical and neurophysiological bases, and computational costs. Edge detectors describe only the edge strength and direction at the rather fine level of neighbouring pixels, requiring various subsequent heuristics to link together edge elements and to extract the desired features (straight lines, open curves, contours, shape boundaries, etc.)

Verlag Ferdinand Berger & Söhne Ges.m.b.H., Horn, Austria, download unter www.biologiezentrum.

Fig. 2B – Smoothed Fig. 2A.

A number of image analysis systems have been developed which automate the identification and/or measurement of biomedical structures. Brenner & al. (1977) classified normal and abnormal leucocytes using pattern recognition methods. Segmentation involved histogram thresholding and heuristic contour search (Brenner & al., 1974, 1981). Bacus & Weens (1977) and Zajicek & Shohat (1983) described computer systems which classified red blood cells with respect to different disorders. Chromosome analysis systems able to

Verlag Ferdinand Berger & Söhne Ges.m.b.H., Horn, Austria, download unter www.biologiezentrum.

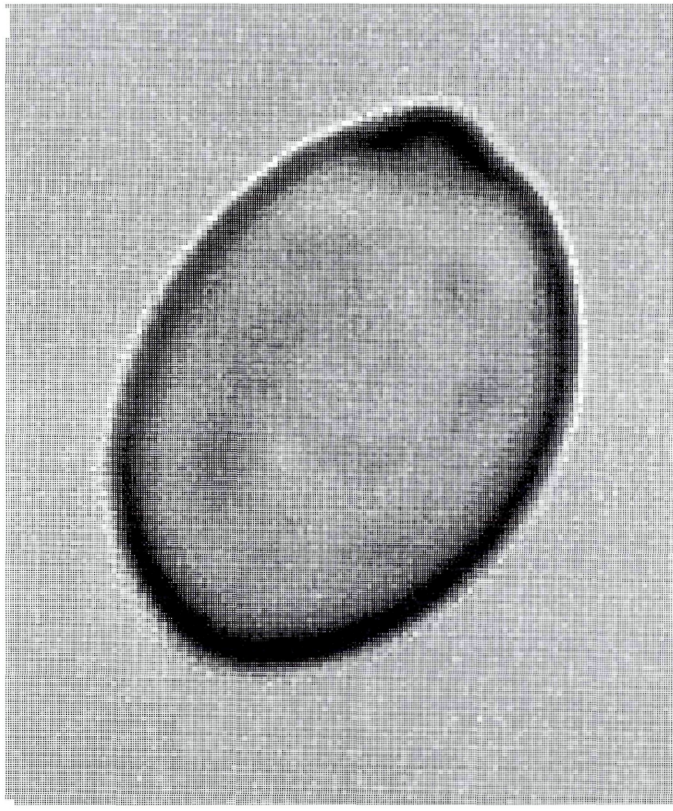

Fig. 2C – Sharpened Fig. 2A.

count, karyotype, and examine bandings, pairings, and abnormalities have been extensively documented (ONOE & al., 1973; VANDERHEYT & al., 1979, 1980, 1981; KLIMENT & al., 1983). Other related topics include the tracing of neurons (CAPOWSKI & SEDIVEC, 1981; SELFRIDGE, 1986) and arteries (KINDELAN & SUAREZ DE LEZO, 1984; REIBER & al., 1984; NGUYAN & SKLANSKY, 1986; SMITH & al., 1986; STEVENSON & al., 1987) through tissue, and the analysis of colon crypt epithelium (ZAJICEK & al., 1982).

Verlag Ferdinand Berger & Söhne Ges.m.b.H., Horn, Austria, download unter www.biologiezentrum.

The development of image processing systems which identify **organisms** appears to have been limited so far to the study of plankton. JEFFRIES & al. (1984) developed a system capable of identifying eight zooplankton taxonomic groups with an accuracy of 90 per cent. The system utilized dark-field illumination and off-normal incident light to facilitate the segmentation of the images by thresholding. Discriminant analysis separated taxonomic groups on a combination of simple features (length, width, area, etc.), and Fourier descriptors and moment invariant features (KATSINIS & al., 1984, 1985). ISHIZUKA & al., (1986) described a similar system which also used thresholding for segmentation and a Fourier-like descriptor to discriminate between two phytoplankton species, *Dinophysis fortii* and *D. acuminata.*

Computer system

The system being used for the present study is a Sun 386i/150 with 8 MB RAM and a 91 MB disk, with an NFS mount to a 500 MB disk. The system is running SunOS 4.0 (4.3 BSD UNIX) and MS-DOS. In the computer is a TrueVision Targa M8 digitizing board which digitizes the video signal coming in from a black and white video camera mounted on a microscope. All software is running under UNIX and is written completely in standard **C** (KERNIGHAN & RITCHIE, 1978). Images are stored in the **IM** format (PAETH, 1986), with programs allowing conversion to other common image formats.

Image processing

The original image is digitized several times, producing 512 × 480 images, differing only in their noise. These images consist of gray levels between 0 and 255, inclusive. These gray levels represent intensities in the original image, with 0 being the darkest (black) and 255 being the brightest (white). Preprocessing involves transforming these images using Principal Component Analysis (GONZALEZ & WINTZ, 1987) to produce one image with a greatly reduced noise content which is used in subsequent processing. This method was found to produce superior image quality compared to both image smoothing and image sharpening. Segmentation of the image is an edge-based, heuristic contour extraction method. The extraction of the subject's contours is broken down into four steps: edge detection, contour edge extraction, edge linking, and line linking. Edge detection examines the differences in the gray levels of pixels in the local neighbourhood of the pixel being examined and calculates an edge strength and direction. Contour edge extraction examines each pixel and, depending on how well the pixel fits the characteristics of a contour point based on its edge direction and strength, places the

Verlag Ferdinand Berger & Söhne Ges.m.b.H., Horn, Austria, download unter www.biologiezentrum.

pixel one of three categories : rejected, possible, or strong. Edge linking builds contours and partial contours by stringing together contiguous strong edges. Line linking links together line segments into larger partial contours toward the building of a completed contour.

(a) SOBEL MASKS

$$\begin{bmatrix} 1 & 2 & 1 \\ 0 & 0 & 0 \\ -1 & -2 & -1 \end{bmatrix} \quad \begin{bmatrix} 2 & 1 & 0 \\ 1 & 0 & -1 \\ 0 & -1 & -2 \end{bmatrix} \quad \begin{bmatrix} 1 & 0 & -1 \\ 2 & 0 & -2 \\ 1 & 0 & -1 \end{bmatrix} \quad \begin{bmatrix} 0 & -1 & -2 \\ 1 & 0 & -1 \\ 2 & 1 & 0 \end{bmatrix}$$

Direction 0 Direction 1 Direction 2 Direction 3

$$\begin{bmatrix} -1 & -2 & -1 \\ 0 & 0 & 0 \\ 1 & 2 & 1 \end{bmatrix} \quad \begin{bmatrix} -2 & -1 & 0 \\ -1 & 0 & 1 \\ 0 & 1 & 2 \end{bmatrix} \quad \begin{bmatrix} -1 & 0 & 1 \\ -2 & 0 & 2 \\ -1 & 0 & 1 \end{bmatrix} \quad \begin{bmatrix} 0 & 1 & 2 \\ -1 & 0 & 1 \\ -2 & -1 & 0 \end{bmatrix}$$

Direction 4 Direction 5 Direction 6 Direction 7

(b) EDGE DIRECTIONS

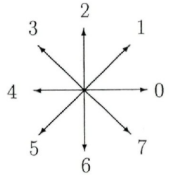

Fig. 3 – Sobel Masks with associated directions.

Preprocessing

Preprocessing of the several incarnations of the image is performed using Principal Component Analysis (PCA, also known as the Hotelling transform and the Karhonen-Loeve transform; Yu & Johanson, 1981; Gonzalez & Wintz, 1987). If the original image can be viewed as a function of x and y, ***f(x,y)***, the digitized image as ***g(x,y)***,

Verlag Ferdinand Berger & Söhne Ges.m.b.H., Horn, Austria, download unter www.biologiezentrum.

and the noise as $n(x,y)$, then each of the images can be described as follows:

$$
\begin{aligned}
g_1(x,y) &= f(x,y) + n_1(x,y) \\
g_2(x,y) &= f(x,y) + n_2(x,y) \\
g_3(x,y) &= f(x,y) + n_3(x,y) \\
&\ldots etc
\end{aligned}
$$

The digitized images, $g_i(x,y)$, are comprised of a sum of identical image terms, $f(x,y)$, and different noise terms, $n_i(x,y)$. PCA takes advantage of the correlation of the original image that exists between the digitized images. A covariance matrix is constructed from the digitized images and the eigenvectors and eigenvalues of this matrix are calculated using the Jacobi Rotation method (WILKINSON, 1972). The eigenvectors are used to transform the digitized images. Of the images produced by this transformation, only the one corresponding to the largest eigenvalue is of interest, as it concentrates the dominant correlated information in the digital images. The other image(s) produced contain(s) much of the noise .

SOBEL MASK

$$
\begin{array}{ccc}
1 & 2 & 1 \\
0 & 0 & 0 \\
-1 & -2 & -1
\end{array}
\qquad
\xrightarrow{\text{CONVOLUTION}}
\qquad
\begin{array}{ccc}
47 & 90 & 52 \\
0 & 0 & 0 \\
-46 & -101 & -47
\end{array}
$$

$$
\begin{array}{ccc}
47 & 45 & 52 \\
49 & 46 & 51 \\
46 & 51 & 47
\end{array}
$$

PIXEL NEIGHBOURHOOD

$$
\begin{aligned}
\text{Edge Strength} &= |47 + 90 + 52 + 0 + 0 \\
&\quad +0 - 46 - 101 - 47| \\
&= |-5| \\
&= 5
\end{aligned}
$$

Fig. 4A – Convolution of direction 0 Sobel mask with relatively uniform image area.

Verlag Ferdinand Berger & Söhne Ges.m.b.H., Horn, Austria, download unter www.biologiezentrum.

SOBEL MASK

$$\begin{matrix} 1 & 2 & 1 \\ 0 & 0 & 0 \\ -1 & -2 & -1 \end{matrix}$$

$$\begin{matrix} 46 & 44 & 47 \\ 53 & 54 & 51 \\ 59 & 64 & 61 \end{matrix}$$

PIXEL NEIGHBOURHOOD

$$\xrightarrow{\text{CONVOLUTION}} \begin{matrix} 46 & 88 & 47 \\ 0 & 0 & 0 \\ -59 & -128 & -61 \end{matrix}$$

$$\begin{aligned} \text{Edge Strength} &= |46 + 88 + 47 + 0 + 0 \\ &\quad +0 - 59 - 128 - 61| \\ &= |-67| \\ &= 67 \end{aligned}$$

Fig. 4B – Convolution of direction 0 Sobel mask with relatively high-contrast area.

Edge detection

The Sobel operator (DOUGHERTY & GIARDINA, 1987) is used to calculate the edge direction and edge strength of each pixel in the image. This edge detector is a computationally inexpensive but effective technique used extensively in biomedical image processing. It consists of eight 3x3 masks, each associated with one of the eight cardinal compass points (Fig. 3). Each of these masks is convoluted with the entire image. Convolution involves the overlay of each Sobel mask over the 3x3 neighbourhood of the pixel being examined. Corresponding values in each of the 3x3 areas are multiplied and these values are summed, and the absolute value taken (Fig. 4). This value is the edge strength at the given pixel in the direction of the mask used (Fig. 4). The edge strengths of the 8 masks are calculated and compared. The edge strength and direction of the mask which produces the largest edge strength is recorded. This is repeated for each pixel in the image except for a one pixel border around the edge of the image whose edge strength is set to zero and whose edge direction is set to null, as the Sobel edge detector requires any pixel being examined to have a complete 3x3 neighbourhood. Fig. 5 shows the normalized edge strength derived using this method.

Verlag Ferdinand Berger & Söhne Ges.m.b.H., Horn, Austria, download unter www.biologiezentrum.

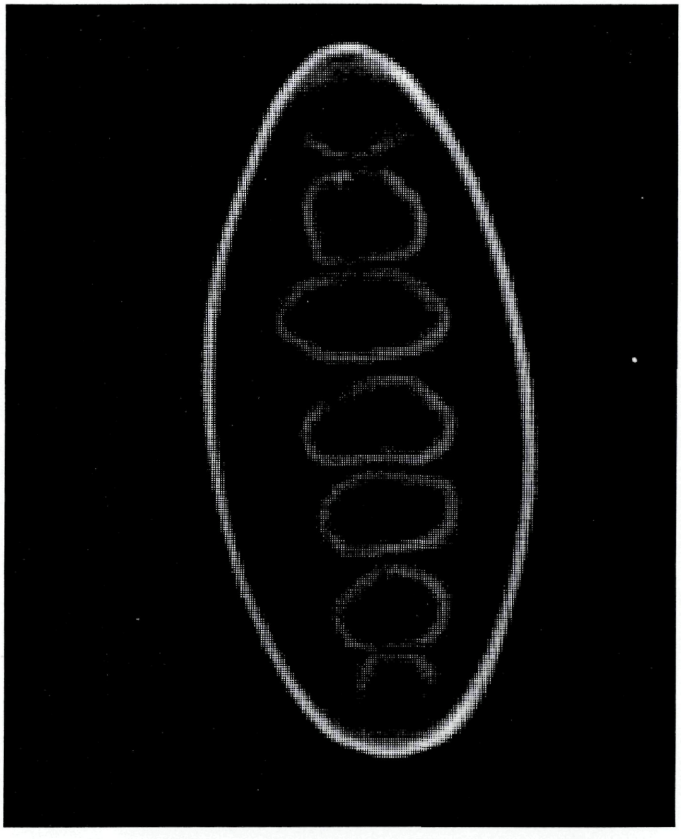

Fig. 5 – Normalized Sobel magnitude of *Bipolaris* image (Fig. 1A).

Contour edge extraction

The edge detection module produces an extensive amount of information which must be reduced in order to make the extraction of contours, which requires the use of higher level, computationally more expensive methods, possible in a reasonable time frame. The actual contours in most images are only a fraction of the total image, so the pixels that are closest to the actual contour are the desired

Verlag Ferdinand Berger & Söhne Ges.m.b.H., Horn, Austria, download unter www.biologiezentrum.

output of this module. In order to extract the edge elements of these contours, an ideal contour in an ideal image is used to model the attributes of edge elements in the digitized image. The constituent elements (pixels) of an ideal contour should have the following properties:

1 – as one approaches the ideal contour element from the directions normal to the tangent of the contour, the edge strength should increase until it is maximum at the ideal contour element. This suggests that ideal contour elements are greater than their orthogonal neighbours (their neighbours in the normal direction – Fig. 6A).

2 – the immediate neighbours orthogonal to the ideal contour element should have the same edge direction as the element. Ideal contour elements should have edge directions which point more or less smoothly in direction of the next ideal edge contour.

This model of how the elements of an ideal edge contour should behave is used to extract pixels which are labelled **Possible** edge contour elements. The following tests are used to both refine and reduce the data set to a set of pixels which have the properties described above for an ideal contour in an ideal image as well as being close to the contour in the real image:

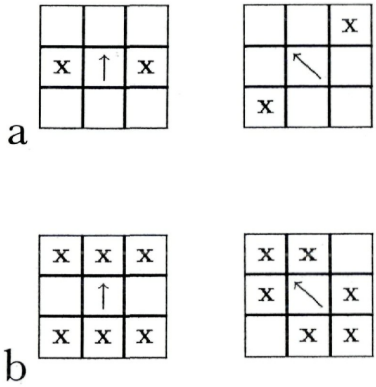

Fig. 6. – A. Neighbours orthogonal (normal) to the pixel edge direction. – B. Neighbours in front of, and behind, the pixel edge direction.

Verlag Ferdinand Berger & Söhne Ges.m.b.H., Horn, Austria, download unter www.biologiezentrum.

1 – pixels whose edge strengths are less than the edge strengths of their two orthogonal neighbours (Fig. 6A) are rejected.

2 – pixels whose two orthogonal neighbours are not in the same direction as the pixel are rejected.

3 – pixels which do not have at least one neighbour in front of ±45°, or behind ±45°) which have the same edge direction ±45°) (Fig. 6B) are rejected.

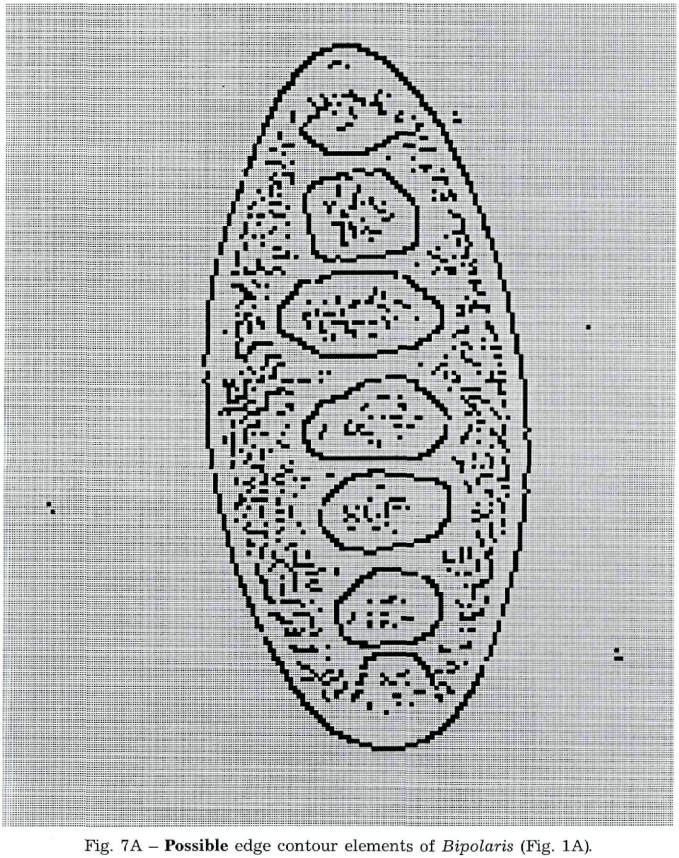

Fig. 7A – **Possible** edge contour elements of *Bipolaris* (Fig. 1A).

Verlag Ferdinand Berger & Söhne Ges.m.b.H., Horn, Austria, download unter www.biologiezentrum.

The **Possible** edge list is examined (Fig. 7A) and all members having an edge strength greater than threshold, **T**, are placed into a second list, **Strong** (Fig. 7B). This is done to further reduce the data set, as many non-contour pixels pass the above three tests because unwanted variation is produced by optical errors and electronic and digitization noise. The threshold T is calculated by multiplying the average of all the Possible edge strengths by a constant, K, in this case 0.45. Other types of images may require experimentation with this constant in order to obtain acceptable results (a more data-dependent method for automatically choosing K is being examined).

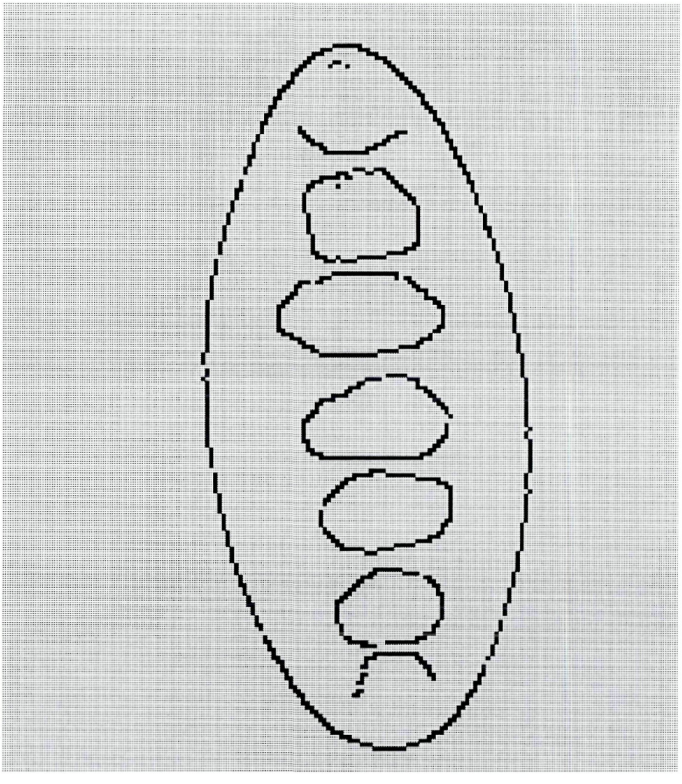

Fig. 7B – **Strong** edge contour elements of *Bipolaris* (Fig. 1B).

Verlag Ferdinand Berger & Söhne Ges.m.b.H., Horn, Austria, download unter www.biologiezentrum.

Edge linking

The Contour Edge Extraction module produces a list of pixels which have a high probability of being on the actual contours being searched for, but does not link them together into contours and partial-contours (line segments). This is done by the Edge Linking module, by expanding in all directions the strong neighbours of a starting Strong pixel:

Begin.
Start a list which is going to contain the contour lists.
While the strong list is not empty.
  Begin.
  Clear the neighbour list.
  Start a new contour list.
  Take the first pixel from the strong list and put it on the top of the neighbour list.
  While the neighbour list is not empty.
    Begin.
    Take the first pixel from the neighbour list and place it in the contour list.
    Examine all of the neighbour pixels and place all strong neighbours into the neighbours list.
    End.
  Insert the contour list into the list of contour lists.
  End.
End.

This routine also notes whether pixels are at the ends of contour segments or are branch points where the contour splits. These points are important, because end points are where the heuristic line-linking algorithm begins its search for the next line to link to in the contour.

Line-linking

The Edge-linking module produces 4 types of contiguous pixel segments:

1 – segments having no split points and no endpoints. These correspond to complete closed contours with no branches.

2 – segments with one or more split points and no end points. These correspond to closed contours with closed branches.

Verlag Ferdinand Berger & Söhne Ges.m.b.H., Horn, Austria, download unter www.biologiezentrum.

3 – segments with no split points and 2 end points. These are simply line segments and correspond to open contours which, with further processing may be found to be closed contours like **1** or **2**, above.

4 – segments with one or more split points and one or more endpoints. These are incomplete contours which may have closed portions and/or many branching open portions.

In most of the images examined, segments produced are of type **3** and **1**, with a few of type **2**, and very rarely type **4**. Many of the subject contours are partially completed by two or more type **3** segments having end points in close proximity to one another. The closing contour module attempts to link together segments to produce complete closed contours.

This module is divided into two parts; the first part (Close) attempts to link together segments whose end points are relatively close together (less than 6 pixels apart); the second method (Distant) attempts to close gaps between segment end points. The Close part begins by running through the contour list and finding the largest contour that it has not searched already and finding the end points of this contour. Beginning with the end point with the largest edge strength, the distance from the end point to all other end points of all contours is calculated. The closest point is chosen to be the goal. A search strategy known as **A*** (NILSSON, 1980; WINSTON, 1984) tries to find the best path (if one exists) linking the starting point to the goal. It expands from the starting point, examining each neighbour of the starting point and, if it is acceptable (having a minimum edge strength), is placed on the **Fringe** list (the **Fringe** list is the list of points on the expanding fringe of the search space). The **Fringe** list is now examined, and the point which is most likely to be on the path is chosen to be the current point. Its neighbours are each examined and placed on the **Fringe** list if they are acceptable. This continues until the goal is reached, or the search goes further than a specified distance (7 pixels) from the start point. How the current point is chosen from **Fringe** list is how the **A*** search differs from other search strategies, such as Depth-first, Branch-and-bound and Hill-climbing (NILSSON, 1980; WINSTON, 1984). The current point is chosen by an heuristic which is based on the cost of the path up to the current point, and an estimate of the cost of the path from the current point to the goal is. Formally:

$$f(n) = g(n) + h(n)$$

Verlag Ferdinand Berger & Söhne Ges.m.b.H., Horn, Austria, download unter www.biologiezentrum.

Where ***f(n)*** is the cost of the adding the current point, ***n***, to the path, ***g(n)*** is the cost of the path leading up to ***n***, and ***h(n)*** is an estimate of the cost from ***n*** to the goal.

```
Begin
Add start to fringe list.
current-point = start.
While fringe list is not empty
  Begin search
  Find the 3 neighbours of the current-point in front of the edge
  direction and add them to the fringe list.
  If any of the 3 neighbours is the goal
    Stop search
  Else
    Begin
    Remove search-node from the fringe list.
    Sort the fringe list based on f().
    current-point = top of fringe list.
    End
  End
End search
```

If a path to the goal is found, the start contour, the path and the goal contour are merged. If this new contour has any end points, the search continues from these; if not, the contour is marked as searched by this part of the module, and the next contour is selected from the list.

The Distant part of the line-linking module is quite similar to the Close part, except that end points more distant than 6 pixels from the start point are considered, the search is allowed to continue deeper, and a more conservative criterion (greater edge magnitude) for adding expanded points to the **Fringe** list is used.

The contour extraction algorithm is very successful in producing the complete outline of the subject. Fig. 8 shows each step in the process of extracting the contours of an ascospore of *Podospora*. This is a rather simple subject with little internal structure. Fig. 9 shows the the final extraction for a conidium of *Bipolaris*, a more complex, darkly pigmented structure with transverse internal septa. The algorithm failed to discriminate the end septa because there is a concentration of pigment at each end of the spore which greatly reduces contrast and makes edge detection almost impossible. The contours for these septa are well defined on their side facing inward, but blend into the outline of the spore on their outer face. This is where the higher cognitive abilities of a human, able to infer a continuous

Verlag Ferdinand Berger & Söhne Ges.m.b.H., Horn, Austria, download unter www.biologiezentrum.

Fig. 8A – Digitized *Podospora* ascospore.

Verlag Ferdinand Berger & Söhne Ges.m.b.H., Horn, Austria, download unter www.biologiezentrum.

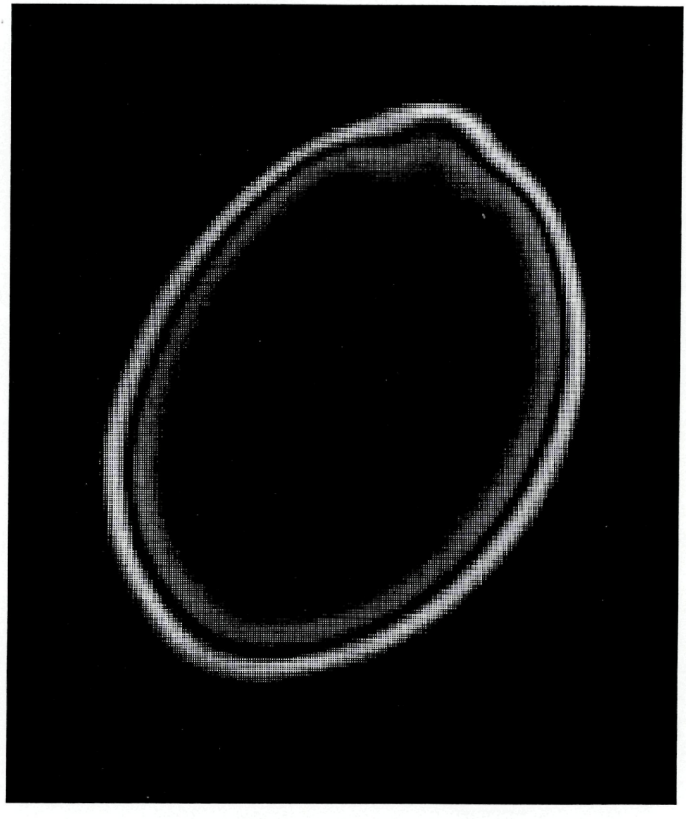

Fig. 8B – Normalized Sobel magnitude of Fig. 8A.

Verlag Ferdinand Berger & Söhne Ges.m.b.H., Horn, Austria, download unter www.biologiezentrum.

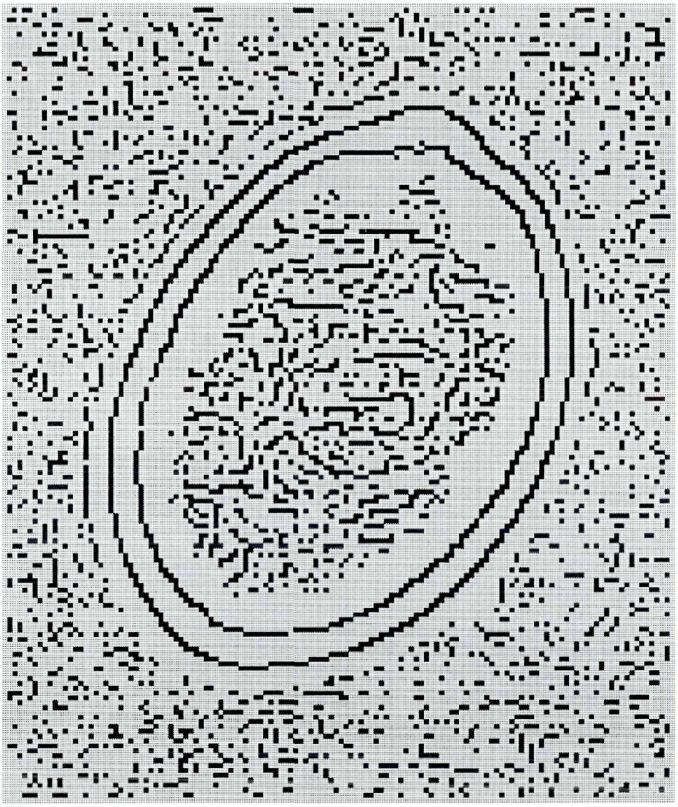

Fig. 8C – **Possible** edge contour elements of Fig. 8A.

Verlag Ferdinand Berger & Söhne Ges.m.b.H., Horn, Austria, download unter www.biologiezentrum.

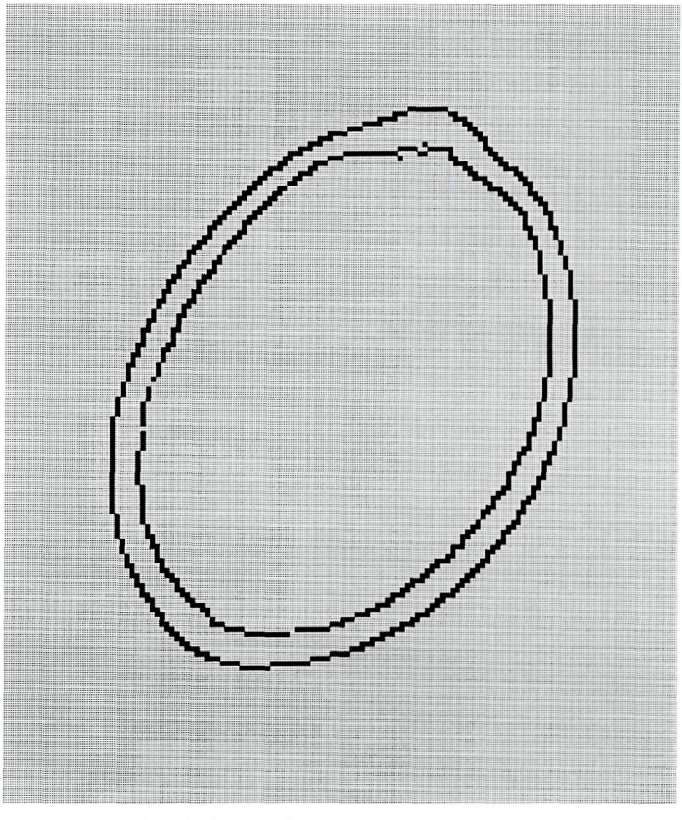

Fig. 8D – **Strong** edge contour elements of Fig. 8A.

Verlag Ferdinand Berger & Söhne Ges.m.b.H., Horn, Austria, download unter www.biologiezentrum.

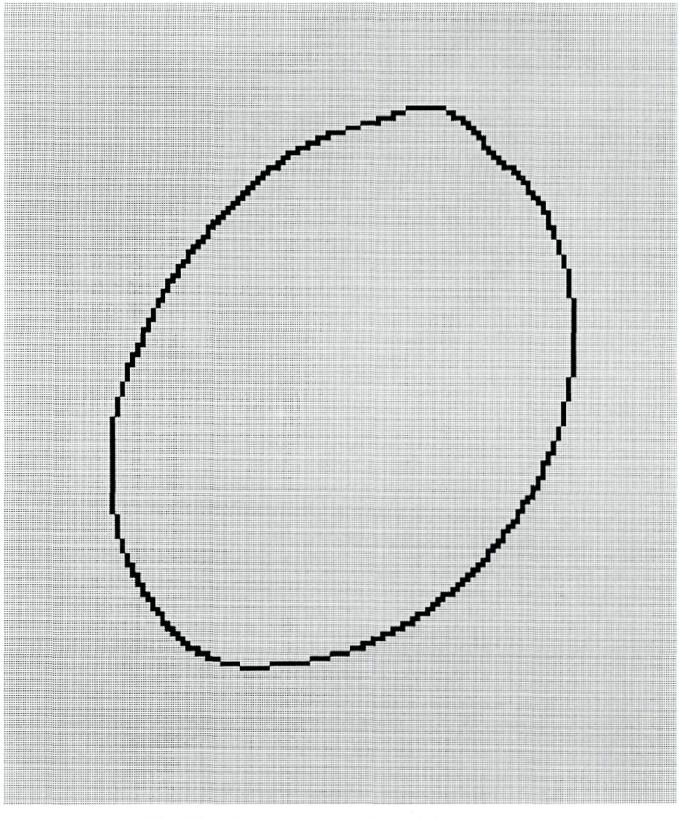

Fig. 8E – Final contours extracted from Fig. 8A.

Verlag Ferdinand Berger & Söhne Ges.m.b.H., Horn, Austria, download unter www.biologiezentrum.

outline where one cannot really be seen, cannot (yet) be emulated by computer. The internal structure of most conidia is not as successfully rendered as the outline of the spore, due to the increased noise introduced by the blurring effect of the part of the spore which is out of the focal plane. The algorithm is also less successful in dealing with contours which involve a great deal of branching, which is often what is produced by the out of focus blurring.

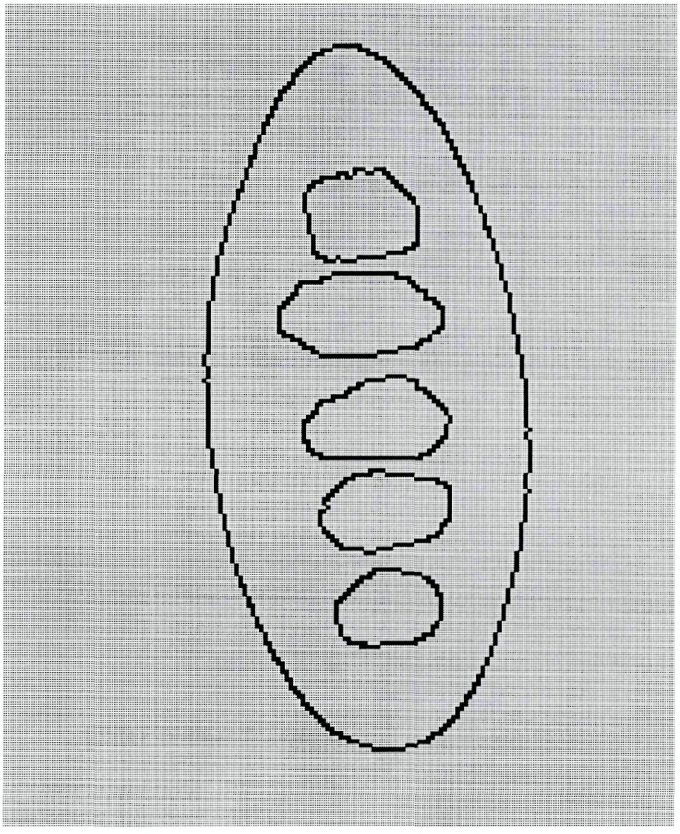

Fig. 9 – Final contours extracted from *Bipolaris* (Fig. 1A).

Verlag Ferdinand Berger & Söhne Ges.m.b.H., Horn, Austria, download unter www.biologiezentrum.

Once the outline of the spore is extracted, specific measurements may be taken. For roughly elliptical shapes, the long and short axes may be calculated by taking the eigenvectors of the shape, and from these the lengths and widths. For more complex shapes, like the conidia of *Helicosporium* and other genera, this method may be inappropriate, as it finds the length along the long axis which may not coincide with the actual spore length.

The information made available by the contour extraction algorithm may now be passed to a data-base being constructed by the taxonomist for the subject organism, or may be passed to an expert system, either for identification or for integration into its knowledge-base (ATKINSON & GAMMERMAN, 1987; PETRINI & RUSCA, 1989). The great amount and complexity of information made available on the subject by image processing makes the use of expert systems more attractive, if not a necessity. The task of identification, from feature extraction to knowledge-based decision making may soon be possible by computer.

Acknowledgments

We would like to thank the PAMI Lab, University of Waterloo, for the initial use of computer equipment. D. NEWTON assisted in the conceptual debugging of various parts of the software, and MARIKA EGYED contributed to the development of this manuscript. We thank the Natural Sciences and Engineering Council of Canada for financial support both in the form of an Operating Grant, and for an Equipment Grant for the purchase of the computer hardware.

References

ATKINSON, W. D. & A. GAMMERMAN (1987). An application of expert systems technology to biological identification.– Taxon 36:705–714.

BACUS, J. W. & J. H. WEENS (1977). An automated method of differential blood cell classification with application to the diagnosis of anaemia.– J. Histochem. Cytochem. 25:614–632.

BALLARD, D. H. & C. M. BROWN (1982). Computer Vision.– Prentice-Hall, Englewood Cliffs, New Jersey.

BRENNER, J. F., E. S. GELSEMA, T. F. NECHELES, P. W. NEURATH, W. D. SELLES & E. VASTOLA (1974). Automated classification of normal and abnormal leukocytes.– J. Histochem. Cytochem. 22(7):697–706.

BRENNER, J. F., T. F. NECHELES, I. A. BONACOSSA, R. FRISTENSKY, B. A. WEINTRAUB & P. W. NEURATH (1977). Scene segmentation techniques for the analysis of routine bone marrow smears from acute lymphoblastic leukemia patients.– J. Histochem. Cytochem. 25(7):601–613.

BRENNER, J. F., J. M. LESTER, W. D. SELLES (1981). Scene Segmentation in Automated Histopathology: Techniques Evolved From Cytology.– Patt. Recog. 13:65–77.

CAPOWSKI, J. & M. SEDIVEC (1981). Accurate computer reconstruction and graphics display of complex neurons utilizing state-of-the-art interactive techniques.– Comput. Biomed. Res. 14:518–532.

Verlag Ferdinand Berger & Söhne Ges.m.b.H., Horn, Austria, download unter www.biologiezentrum.

DOUGHERTY, E. R & G. R. GIARDINA (1987). Image Processing – Continuous to Discrete Vol.1: Geometric, Transform, and Statistical Methods.– Prentice-Hall, Englewood Cliffs, New Jersey.

FU, K. S. & J. K. MUI (1981). A Survey of Image Segmentation.– Patt. Recog. 13:3–16.

GONZALEZ, G. C. & P. WINTZ (1987). Digital Image Processing. 2nd edn.– Addison-Wesley, Reading, Mass.

GRANRATH, D. J. (1981). The role of human visual model in image processing.– Proc. IEEE 69:552–561.

HARALICK, R. M (1984). Digital Step Edges from Zero Crossing of Second Directional Derivatives.– IEEE Trans. PAMI 6:58–68.

HARALICK, R. M. & L. G. SHAPIRO (1985). Image Segmentation Techniques.– Comput. Vision Graphics Image Process. 29:100–132.

HILDRETH, E. C. (1983). The detection of intensity changes by computer and biological vision systems.– Comput. Vision Graphics Image Process. 22:1–27.

ISHIZUKA, M, K. TSUBOI & M. OHGUSHI (1986). Pattern recognition of dinophysis of oceanic phytoplankton.– Proc. 8th Intnl. Conf. Patt. Recog. pp. 540–542, Paris, France.

JEFFRIES, H. P, M. S. HERMAN, A. D. POULARIKAS, C. KATSINIS, I. MELAS, K. SHERMAN & L. BIVINS (1984). Automating size, counting and identification of zooplankton by pattern recognition.– Mar. Biol. 78:329–334.

KATSINIS, C., A. POULARIKAS & H. JEFFRIES (1984). Image processing and pattern recognition with applications to marine biological images. In: TESCHER, A.G.(ed.) Applications in Digital Image Processing VII.– SPIE Vol.504. SPIE 28th Ann. Intl. Tech. Symp. Optics and Electro-optics, August 21–24, 1984, San Diego, Calif.

KATSINIS, C., A. POULARIKAS & H. JEFFRIES (1985). A perimetric sampling technique applied to biological images. In: TESCHER, A.G.(ed.) Applications of Image Processing VIII.– SPIE Vol.575. SPIE 28th Ann. Intl. Tech. Symp. Optics and Electro-optics, August 20–22, 1985, San Diego, Calif.

KERNIGHAN, B. W & D. M. RITCHIE (1978). The C Programming Language. – Prentice-Hall, Englewood Cliffs, New Jersey.

KINDELAN, M. & J. SUAREZ DE LEZO. 1984. Artery detection and tracking in coronary angiography. In Digital Image Analysis, Eds. Levialdi.– Pitman, London.

KLIMENT, V., R. TUSCANY, J. DVORAK, L. TOMASEK (1983). Computer-assisted analysis of human G-banded chromosomes.– Comput. Biomed. Res. 16:20–28.

MARR, D. & E. Hildreth (1980). Theory of Edge Detection.– Proc. R. Soc. Lond B 207:197–217.

NGUYEN, T. V., J. SKLANSKY (1986). Computing the Skeleton of Coronary Arteries in Cineangiograms.– Comput. Biomed. Res. 19:428–444.

NILSSON, N. J. (1980). Principles of Artificial Intelligence.– Tioga Publ. Palo Alto, California.

ONOE, M., M. TAKAGI & K. YUKIMATSU (1973). Chromosome Analysis by Minicomputer.– Comput. Vision Graphics Image Process. 2:402–416.

PAETH, A. W. (1986). The IM Raster Toolkit Design, Implementation and Use.– Technical Report CS-86-65, Computer Science Department, University of Waterloo, Waterloo.

PAVLIDIS, T. (1978). A Review of Algorithms for Shape Analysis.– Comput. Graphics Image Process. 7:243–258.

PERSOON, E. & K. S. FU (1977). Shape discrimination using Fourier descriptors.– IEEE Trans. PAMI 8:388–397.

PETRINI, O. & C. RUSCA (1989). Knowledge-based expert systems in mycology: tolerance is a necessary attribute.– The Mycologist 3:128–130.

REIBER, J. H. C., C. J. KOOIJMAN, C. J. SLAGER, J. J. GERBRANDS, J. C. H. SCHUURBIERS, A. D. BOER, W. WIJNS, P. W. SERRUYS & P. G. HUGENHOLTZ (1984). Coronary Artery

Verlag Ferdinand Berger & Söhne Ges.m.b.H., Horn, Austria, download unter www.biologiezentrum.

Dimensions from cineangiograms-Methodology and Validation of a Computer-assisted Analysis Procedure.– IEEE Trans. Med. Imag. 3:131–139.

SAHOO, P. K., S. SOLTANI, A. K C. WONG & Y. C. CHEN (1985). A Survey of thresholding techniques.– Comput. Vision Graphics Image Process. 41:233–260.

SELFRIDGE, P. G. (1986). Locating Neuron Boundaries in Electron Micrograph Images Using "Primal Sketch" Primitives.– Comput. Vision Graphics Image Process. 34:156–165.

SMITH, L. D. R., G. ROBINSON, D. STEVENSON, H. SANGHERA & P. QUARENDON (1986). Proc. Second Int. Conf. Image Process. & Applics. pp. 72–76.– 24–26 June, 1986, London.

STEVENSON, D. J., L. SMITH & G. ROBINSON (1987). Working towards the automatic detection of blood vessels in X-ray angiograms.– Patt. Recog. Lett. 6:107–112.

VANDERHEYDT, L., F. DOM, A. OOSTERLINCK, H. VAN DEN BERGHE (1979). Design of a Special Interpreter for the Classification of Human Chromosomes.– IEEE Trans. PAMI 1:214–219.

VANDERHEYDT, L., A. OOSTERLINCK, J. VAN DAELE, H. VAN DEN BERGHE (1980). Design of a graph-representation and a fuzzy-classifier for human chromosomes.– Patt. Recog. 2:201–210.

VANDERHEYDT, L., F. DOM, A. OOSTERLINCK, H. VAN DEN BERGHE (1981). Two-Dimensional Shape Decomposition Using Fuzzy Subset Theory Applied To Automated Chromosome Analysis.– Patt. Recog. 13:147–157.

WATT, R. J. (1987). An outline of the primal sketch in human vision.– Patt. Recog. 5:139–150.

WILKINSON, J. H. (1972). Handbook for Automatic Computation Vol II: Linear Algebra.– Springer-Verlag, Berlin.

WINSTON, P. A. (1984). Artificial Intelligence.– Addison-Wesley Pub. Reading, Massachusetts.

YU, Y. S. & P. JOHANSEN (1981). Digital Image Processing of Multi Spectral Images.– Rapport 81/1, Institute of Datalogy, University of Copenhagen.

ZAJICEK, G., H. P. MEINZER, D. KOMITOWSKI (1982). Automated Image Processing of the Colon Crypt Epithelium.– Comput. Biomed. Res. 15:155–163.

ZAJICEK, G. & M. SHOHAT (1983). On the Classification of Nucleated Red Blood Cells.– Comput. Biomed. Res. 16: 553–562.

ZOBODAT - www.zobodat.at

Zoologisch-Botanische Datenbank/Zoological-Botanical Database

Digitale Literatur/Digital Literature

Zeitschrift/Journal: Sydowia

Jahr/Year: 1990

Band/Volume: 42

Autor(en)/Author(s): Newton G., Kendrick B.

Artikel/Article: Image processing in taxonomy. 246-272